

## **Prediction of rib cage fracture in computational modeling: effect of rib cortical thickness distribution and intercostal muscles mechanical properties**

D. Subit, M. Kindig, Z. Li, R. Kent, Center for Applied Biomechanics, Univ. of Virginia, USA  
P. Baudrit, Centre Européen d'Etudes de Sécurité et d'Analyse des Risques, France  
M. Jansova, L. Hyncik, University of West Bohemia, Czech Republic  
T. Dziewonski, J. Toczyski, University of Warsaw, Poland

*This paper has not been screened for accuracy nor refereed by any body of scientific peers  
and should not be referenced in the open literature.*

### **ABSTRACT**

*A finite element model of the 50<sup>th</sup> percentile male was developed based on geometrical surface generated from medical images. First, an interactive multi-block meshing approach was used to generate high quality quadrilateral and hexahedral meshes of the thorax anatomical structures. Second, a methodology based on the mesh blocks was developed to assign cortical thickness data taken from a micro-CT study to each of the nodes in the cortical shell elements of the ribs along the longitudinal direction and around the cross-sectional perimeter. The whole thorax model (rib cage, internal organs, muscles, skin) was exercised under a wide range of loadings that include inertial and non inertial loadings (blunt impacts, and table top). Although the response of the thorax model was reasonable compared to the experimental results at a “global” level—such as under hub or belt loading onto the entire body—, it has not been evaluated at a local level -- such as the strain distribution in the rib cage. The structural response of the rib cage was therefore investigated to evaluate the effect of cortical thickness distribution and intercostal muscle mechanical properties on the thorax mechanical response. The need for node dependent cortical thickness to predict force and deflection at the time of fracture was demonstrated at the rib level by simulating antero-posterior dynamic bending of individual ribs. As for the intercostal muscles, there is no experimental data available to aid with the definition of their mechanical properties. Therefore the impacts to the lateral thorax recently performed by CEESAR for the THOMO project were used to carry out a sensitivity analysis to assess the effect of the cortical thickness distribution and intercostal muscles material properties on rib fracture prediction. The FE model of the thorax was run for three cortical thickness distributions (one distribution with thicknesses defined for each node, and two distributions of uniform thickness values) and three values for the intercostal*

*muscles' Young's modulus. The variation of the strain field was compared for the various combinations of parameters and loading conditions to assess how the fracture prediction was altered. In particular, the rib strain profiles measured in the experiments as well as the locations of the rib fractures were compared to the FE results. This study represents a major effort in the development and validation of the thorax finite element model for the Global Human Body Modeling Consortium, and provides insight for the development of anatomically detailed computational models for injury prediction.*

## INTRODUCTION

Increasingly, computational finite element (FE) modeling is being used to better understand the fracture tolerance and structural response of the chest under a variety of loading conditions. Several major models have been developed, including the LAB/CEESAR model (Lizee *et al.* 1998), the GM model (Deng *et al.* 1999), the Human Model for Safety (HUMOS)(Robin 2001), the Wayne State University model (Wang 1995, Shah *et al.* 2001), the Total Human Model for Safety (THUMS) (Iwamoto *et al.* 2002, Kimpara *et al.* 2005), H-Model (Haug *et al.* 2004), the Takata model (Zhao and Narwani 2005), and the Ford model (Ruan *et al.*, 2003). FE models allow one to simulate thoracic impacts using a wider variety of boundary conditions, material properties, and other variables than would not be possible experimentally due to cost, material availability, instrumentation limitations, or physical constraints. However, because of their complexity and size, and the number of parameters (physical and numerical) that can be adjusted, benchmarking an FE model against experimental data remains an ongoing area of research. Typically these models are validated at a larger-scale “global” level—such as under hub or belt loading onto the entire body—and lack validation on a more local level, such as at the level of an individual ribs. However, fracture prediction at the bone level requires computational model to properly predict the strain distribution as strain is commonly used for fracture prediction. A recent study by Li *et al.* (2010) has shown that the cortical thickness distribution was an important parameter to include in the rib FE model to properly predict force and displacement at fracture under antero-posterior loadings. The modeling approach consisted in mapping rib cortical information obtained from microtomographic images onto the rib surfaces. This approach allowed to include the variation in rib cortical thickness along the rib and around the perimeter of the rib cross-section (Li *et al.*, 2011). However, the need for detailed cortical thickness distribution was not assessed at the ribcage level. In addition, on-going work by Kindig *et al.* (2012) shows that the intercostal muscles contribute substantially to the structural response of the ribcage, but there is no data in the literature to determine the material properties of the intercostal muscles: most of the computational models that include intercostal muscles in injury biomechanics (Wang 1995, Planck and Eppinger 1991, Kimpara *et al.* 2005) use intercostal properties reported by Yamada (1970) for the intercostal muscles. The Yamada study, however, does not specifically identify intercostal material properties, but instead lists properties for other thoracic muscles, such as the pectoralis major and the trapezius—which subsequent studies have used to approximate the intercostal muscle properties. Therefore, the objective of this study was to evaluate the effect of the cortical thickness distribution (CTD) and mechanical properties of the intercostal muscles (IM) on the fracture prediction capabilities of the GHBMC (Global Human Body Modeling Consortium) thorax model (Li *et al.*, 2011). To do so, lateral impact tests recently performed at CEESAR (Centre Européen d'Etudes de Sécurité et d'Analyse des Risques, Leport *et al.*, 2011) were used: three post-mortem human subjects (PMHS) instrumented with strain gauges on the ribs were impacted, and this impact condition was simulated with the GHBMC thorax model for various combination of cortical thickness and Young's modulus for the intercostal muscles. A total of twelve simulations were performed, and the strain distribution in the ribs, and in the intercostal muscles was analyzed. The number of rib fractures as well as their locations was compared to the experiments.

## METHODS

The structural response of the rib cage was investigated to evaluate the effect of cortical thickness distribution and intercostal muscle mechanical properties on the thorax mechanical response. The IM was modeled as a linear elastic material, and a parametric study was carried out with the GHBMC thorax model

to determine the effect of the IM Young's modulus and CTD on fracture prediction. The lateral impactor tests performed in the THOMO project and reported on in Leport et al (2011) were used as reference.

## Experimental data

Three PMHS were subjected to lateral impact (Figure 1). They were seated in an upright position, with the arms up, and the center of the impactor was aligned with the midline of the thorax at the level of the right 6<sup>th</sup> rib. The impactor had a diameter of 152 mm, weighted 23.5 kg, and its initial velocity was 4.4 m/s. The subject was held in position through three positioning straps attached to the head and the arms. The straps were released a few milliseconds prior to the impact.

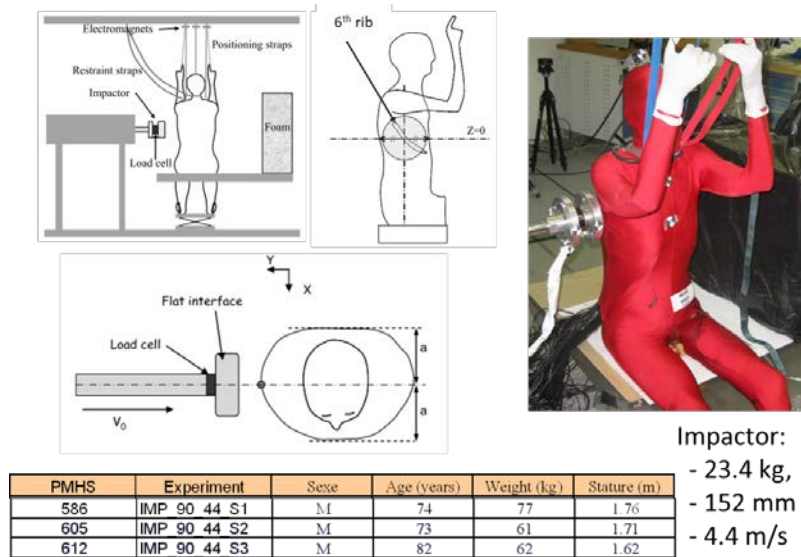


Figure 1: Overview of the test conditions (Leport et al, 2011).

The ribs were bilaterally instrumented with up to six strain gauges. The load in the impactor was measured thanks to a load cell located behind the impactor probe. These sensors were sampled at 10 kHz. After the impacts, necropsies were performed and the number of rib fractures as well as their location was documented.

## FE models and parametric analysis

The detailed GHMBC thorax model was connected to simplified versions of the lower extremities, abdomen, neck and head (Li *et al*, 2010). The arms of the GHMBC model were rotated upward to replicate the impact condition. The FE model of the thorax was run for three CTD (one distribution with thicknesses defined for each node of the mesh, and two distributions of uniform thickness values) and three values for the IM Young's modulus (Table 1). The average value for the model with node-dependent CTD was 0.9 mm. The models were run with rib fracture simulated by deleting elements where the plastic strain of 1.8% was reached.

Table 1: Values for the parametric analysis

		Cortical thickness distribution (mm)			
		Uniform: 0.6	Uniform: 0.8	Node dependent	Uniform: 1
Intercostal muscle (IM) Young's modulus (MPa)	0.21				
	2.1			reference	
	21				

## Strain analysis and corridors development

The strain gauge signals from the experiment were analyzed following the methodology outlined in Trosseille et al (2008). The main steps are summarized below:

- First, each signal was first qualitatively analyzed in order to detect possible problems which could alter the analysis, such as saturation, noise, or null or constant signal,
- Second, the strain profile was determined for each rib ring, by interpolating the strain as a function of the curvilinear abscissa  $s$ ,
- Third, the strains were normalized to allow for the comparison between different tests or rib levels: first, the effective strain,  $\varepsilon_{RMS}$  (RMS stands for Root Mean Square) was calculated for the bilateral costal arcs for each rib level (Equation 1:  $s_1$  and  $s_n$  are the curvilinear abscissa of the first and last strain gauges on either the left or right sides), and second the strain time-history for each strain gauge was divided by the effective strain to obtain the normalized strain  $\varepsilon_N(s, t)$  (Equation 2).

$$\varepsilon_{RMS}(t) = \sqrt{\frac{1}{((s_1 - s_n)_{left} + (s_n - s_1)_{right})} \left( \left( \int_{s_n}^{s_1} (\varepsilon(s, t))^2 ds \right)_{left} + \left( \int_{s_1}^{s_n} (\varepsilon(s, t))^2 ds \right)_{right} \right)} \quad \text{Eq. 1}$$

$$\varepsilon_N(s, t) = \frac{\varepsilon(s, t)}{\varepsilon_{RMS}(t)} \quad \text{Eq. 2}$$

The gauge variation of the strain was analyzed by calculating the mean value and standard deviation of the normalized strains for a time period from 10 to 99% of the time at fracture (or peak strain in the cases where there was no fracture). The curvilinear abscissa  $s$  was defined for the left (for -100% at the costo-chondral junction (CCJ) to 0% at the consto-transverse joint (CTJ)), and right (0% at the CTJ and 100% at the CCJ) ribs (Figure 2). The normalized effective strain was found to capture the type and direction of the impact applied to the thorax (Trosseille et al, 2008).

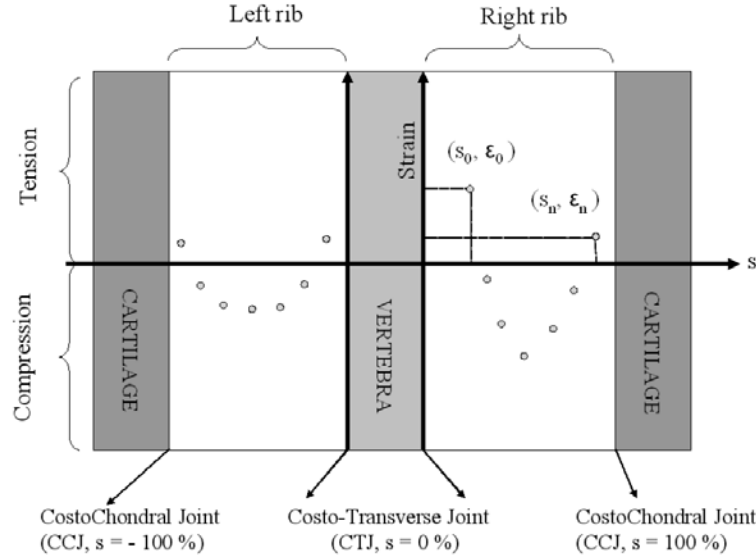


Figure 2: Schematic for the reference coordinate system defined to describe the strain profiles in the ribs (from Trosseille et al, 2008).

The strain along the longitudinal axis of the rib was also determined in the rib FE models. The strain profiles were determined for the all the rib levels, assuming that the strain along the direction of nodes 1 and 2 in the model was comparable to that measured by the strain gages in the experiments (Figure 3). The node connectivity in the mesh of each rib followed this numbering scheme.

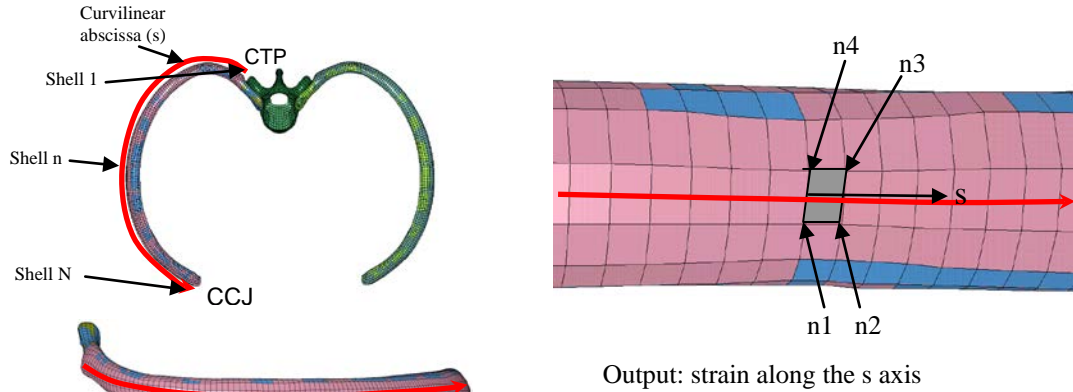


Figure 3: Determination of the strain profiles in the GHBM rib models

## RESULTS and DISCUSSION

### Peak impact force

The peak impact forces were compared to the experimental results and to the ISO corridor for side impact (ISO, 1998) (Figure 4). Overall, the peak forces were greater in the model, and increased with increasing Young's modulus for the IM for each given CTD. The model with node-dependent (ND) CTD was found to be less sensitive to the variation of IM Young's modulus. It is interesting to note that although the IM Young's modulus has an effect on the peak force value, the range of variation is not enough reduce the peak force to a point where it would be within the ISO or experimental ranges.

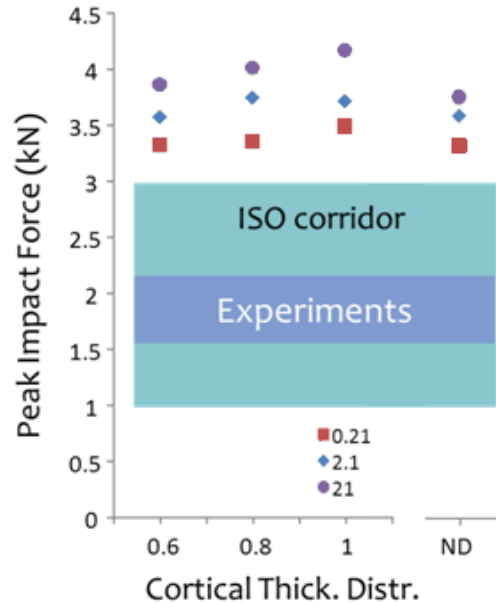


Figure 4: Comparison of the peak impact forces obtained in the simulation to the experiments and ISO corridor. ND: node-dependent.

## Rib fracture

The number of fractured ribs was compared between the simulations and the experiments (Table 2 and Table 3). Significantly more fractures were reported in the experiments than in the simulations, with no fracture reported for the models with uniform CTD of 0.8 and 1 mm. Fractures were observed, for the 0.6 uniform CTD and ND CTD, and the location was found to be sensitive to the IM Young's modulus (Table 4).

Table 2: Fractured ribs for the FE simulations


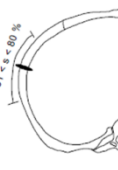
		Cortical thickness distribution (mm)			
		Uniform: 0.6	Uniform: 0.8	Node dependent	Uniform: 1
Intercostal muscle (IM) Young's modulus (MPa)	0.21	Ribs 7, 8	none	Rib 7	none
	2.1	none	none	Rib 4	none
	21	Rib 4	none	Rib 4	none

Table 3: Fractured ribs in the experiments

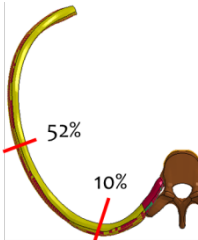
PMHS	Rib level
586	4, 5, 7, 8 (single fracture)
605	4, 6, 7, 8 (single fracture)
612	3, 4, 5, 6, 7, 8, 9 (multiple fracture)

Compared to the experiments, the model indicated significantly fewer fractures for any set of parameters. However the fractures were located around the same location (Table 4), although no rib was fractured in multiple locations in the simulations.

Table 4: Comparison of fracture location between experiments and simulation

Experiment	FE simulations		
	44%	Cortical thickness distribution (mm)	
	24%	Uniform: 0.6	Node dependent
Intercostal muscle (IM) Young's modulus (MPa)	0.21	Rib 7 (11 %) Rib 8 (10%)	Rib 7 (53%)
	2.1	none	Rib 4 (52%)
	21	Rib 4 (52%)	Rib 4 (52%)

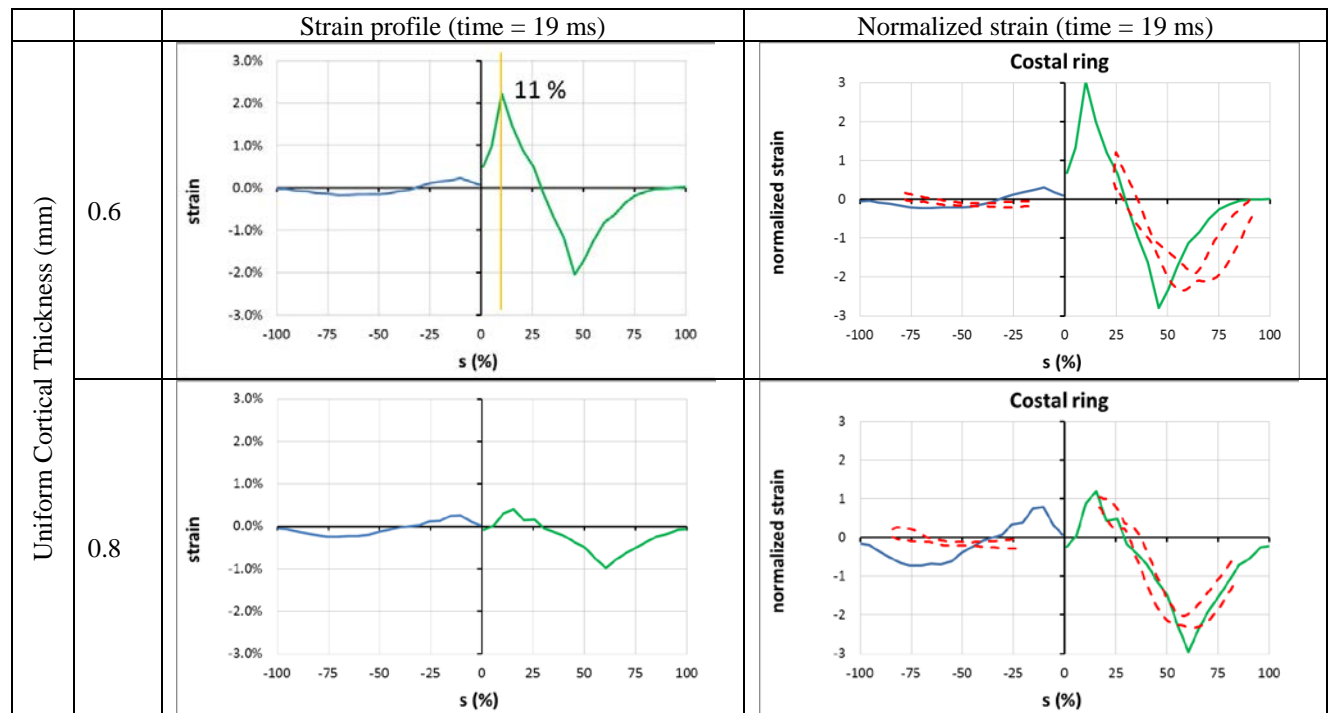
The number in parenthesis indicates the normalized curvilinear abscissa for the fracture location.



## Strain profiles in the ribs

At the strain level, the strain distribution between the left and right sides was consistent with the experiment, with very low deformation on the non-struck side (Table 5). In addition, the response of the models was overall in reasonable agreement with the corridors developed for the normalized strain, published in Leport *et al* (2011), with some variations observed based on the choice of parameters. The strain profiles were compared in the bilateral ribs 7 for the model with cortical thickness of 0.6 and 0.8 mm (Table 5). While the former model predicted a fracture at 19 ms, located at 11% of curvilinear abscissa, no fracture were predicted in the latter model. The normalized strain profiles indicate a better agreement with the model with 0.8 mm of cortical thickness than with the model with 0.6 mm of cortical thickness. However several fractures were reported in the experiments, and none of these models (or any of the models developed in this parametric analysis) predicted that many fractures.

Table 5: Comparison of the strain profiles in the bilateral ribs 7 for two values of uniform cortical thickness. The red dash lines on the normalized strain plots indicate the corridor derived from the experimental data. The vertical line for the model with 0.6 mm thickness indicates the location of fracture. No fracture was obtained for the model with 0.8 mm thickness.



## Effect of the intercostal muscle Young's modulus

The strain fields in the ribs and in the IM were greatly sensitive to the stiffness of the IM (Figure 5). The deformation of the rib cage with ND CTD at a given instant ( $t=19\text{ms}$ ) suggests different rib kinematics based on the IM material properties. For the model with the lowest Young's modulus, the deformation of the rib cage is larger and more localized than for the models with greater Young's modulus. In addition, the fracture location (rib level and location on the rib) depends on the value of the IM Young's modulus.



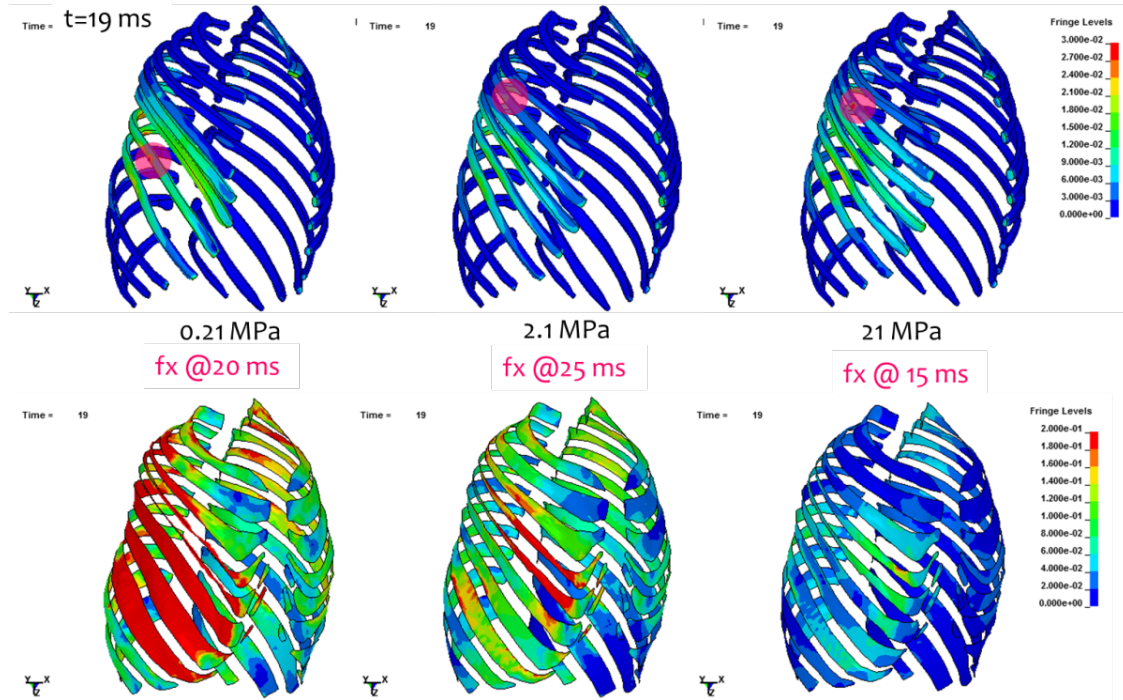


Figure 5: Principal strain in the ribs (top) and intercostal muscles (bottom), for the ND CTD with IM Young's modulus of 0.21 MPa (left), 2.1 MPa (center) and 21 MPa (right). The strain fringe level goes from 0 to 3 % for the ribs, and 0 to 20 % for the IM. The circular shaded area indicates the position of the rib fracture.

## CONCLUSIONS

A rib cage model was developed with ND CTD for the ribs by combining the geometry obtained from clinical CT images (Gayzik *et al*, 2011) and the cortical thickness determined from microCT images (Choi *et al*, 2009). The need for ND CTD to predict force and deflection at the time of fracture was demonstrated at the rib level by simulating antero-posterior dynamic bending of individual ribs, but never evaluated at the rib cage level. The study reported in this paper describes the first attempt to evaluate how the level of details in the rib model affects the number and location of the predicted rib fractures. In addition, this study provides some preliminary results regarding the effect on the intercostal muscles on the structural and injurious response of the rib cage. Although a simple model was used for the IM (linear elastic), the results presented in this study highlights the need for a better characterization of the mechanical response of the IM, as the response of the rib cage is sensitive the mechanical properties of the IM.

## ACKNOWLEDGEMENTS

Financial support in this study was provided by the Global Human Body Models Consortium, LLC (UVA: TM-001) for the modeling portion, and the European Community FP7th for the experimental portion (THOMO project, [www.thomo.eu](http://www.thomo.eu)). The authors would like to acknowledge the contributions of the different partners involved in these projects.

## REFERENCES

- CHOI, Y.C., and Lee, I. (2009). Thorax FE model for older population. Japanese Society of Mechanical Engineers (JSME), Fukuoka
- DENG Y-C., KONG W., AND HO H. (1999) Development of a Finite Element Human Thorax Model for Impact Injury Studies. Society of Automotive Engineers Paper 1999-01-0715, Warrendale, PA.



- GAYZIK, F. S, MORENO, D. P., GEER, C. P., WUERTZER, S. D. MARTIN, R. S. and STITZEL, J. D. (2011), Development of a Full Body CAD Dataset for Computational Modeling: A Multi-modality Approach, *Ann Biomed Eng.* 2011 Oct;39(10):2568-83.
- HAUG E., CHOI H-Y., ROBIN S., AND BEAUGONIN M. (2004) Human Models for Crash and Impact Simulation. In *Handbook of Numerical Analysis*, Vol. 12, Ciarlet P.G., ed., Amsterdam: Elsevier, pp. 297-361.
- ISO/TR9790-3. (1988) Road Vehicles – Anthropomorphic Side Impact Dummy – Lateral Thoracic Impact Response Requirements to Assess the Biofidelity of the Dummy. International Standards Organization, American National Standards Institute, NY
- IWAMOTO M., KISANUKI Y., WATANABE I., FURUSU K., AND MIKI K. (2002) Development of a Finite Element Model of the Total Human Model for Safety (THUMS) and Application to Injury Reconstruction. *Proc. of 2002 International Research Council on the Biomechanics of Impact*, Munich.
- KIMPARA H., LEE J., YANG K., KING A., IWAMOTO M., WATANABE I., AND MIKI K. (2005) Development of a Three-Dimensional Finite Element Chest Model for the 5th Percentile Female. *Stapp Car Crash Journal*, Vol. 49, pp. 251-269.
- KINDIG, M.W., Li, Z., KENT, R.W., and SUBIT, D (in preparation), Effect of Intercostal Muscle and Costovertebral Joint Material Properties on Human Ribcage Stiffness and Kinematics, to be submitted to *Computer Methods in Biomechanics and Biomedical Engineering*.
- LEPORT T, BAUDRIT P, POTIER P, TROSSEILLE X, LECUYER E, VALLANCIEN G, (2011). Study of Rib Fracture Mechanisms Based on the Rib Strain Profiles in Side and Forward Oblique Impact, 55th *Stapp Car Crash Conference*
- LI, Z., KINDIG, M., KERRIGAN, J.W., UNTARIOU, C.D., SUBIT D., CRANDALL, J.R., KENT, R.W., 2010. Rib fractures under anterior-posterior dynamic loads: experimental and finite element study. *Journal of Biomechanics* 2010; 43(2):228-234.
- Li, Z., KINDIG, M.W., SUBIT, D., and KENT, R.W. (2010). Influence of mesh density, cortical thickness and material properties on human rib fracture prediction. *Medical Engineering & Physics*, 32(9), 998-1008.
- LIZEE, E., ROBIN, S., SONG, E., BERTHOLON, N., LECOZ, J.Y., BESNAULT, B., LAVASTE, F., 1998. Development of a 3D finite element model of the human body. *Proc. 42<sup>nd</sup> Stapp Car Crash Conference*, pp. 115-138. Society of Automotive Engineers, Warrendale, PA.
- ROBIN S. (2001) HUMOS: Human Model for Safety—A Joint Effort towards the Development of Refined Human-like Car Occupant Models. *Proc. 17th Enhanced Safety of Vehicles Conference*, Paper 297.
- SHAH C.S., YANG K.H., HARDY W.N., WANG K., AND KING A.I. (2001) Development of a Computer Model to Predict Aortic Rupture due to Impact Loading. *Stapp Car Crash Journal*, Vol. 45, pp. 161-182.
- TROSSEILLE X, BAUDRIT P, LEPORT T, VALLANCIEN G. (2008). Rib cage strain pattern as a function of chest loading configuration. *Stapp Car Crash J.* 2008 Nov;52:205-31.
- WANG H-C.K. (1995) Development of a Side-Impact Finite Element Human Thoracic Model. Ph.D. Dissertation, Wayne State University, Detroit, Michigan.
- Z. LI, D. SUBIT, M.W. KINDIG, R.W. KENT (2010) Development of a Finite Element Ribcage Model of the 50th Percentile Male with Variable Rib Cortical Thickness, *INJURY BIOMECHANICS RESEARCH*, Proceedings of the 38<sup>th</sup> International Workshop.
- ZHAO J. AND NARWANI G. (2005) Development of a Human Body Finite Element Model for Restrain System R & D Applications. *Proc. 19th International Technical Conference on Experimental Safety of Vehicles*.